

Zwitterionic Copolymer-Supported Ionogel Electrolytes Featuring a Sodium Salt/Ionic Liquid Solution

*Huan Qin and Matthew J. Panzer**

Department of Chemical and Biological Engineering, Tufts University

4 Colby Street, Medford, MA 02155

*Corresponding author: matthew.panzer@tufts.edu

Abstract

A series of zwitterionic (ZI) copolymers, including both binary, fully-ZI and ternary, partially-ZI copolymer variations, have been successfully employed as scaffolds to support mechanically robust ionic liquid-based gel (ionogel) electrolytes containing sodium bis(trifluoromethylsulfonyl)imide salt. All of the synthesized ionogels, which were optically transparent and freestanding without any covalent cross-links, contained 15 mol% copolymer and displayed room temperature ionic conductivities above 1 mS cm^{-1} while also exhibiting high compressive elastic modulus values (0.7-11 MPa). The activation energy of ionic conductivity of an ionogel with a fully-ZI copolymer scaffold (18 kJ mol^{-1}) was found to be noticeably lower than that of the ionic liquid electrolyte solution itself (23 kJ mol^{-1}), highlighting the positive role that ZI moieties may play in aiding ion transport. NMR chemical shift analysis revealed favorable interactions between sodium cations and both types of ZI motifs employed here (sulfobetaine and

phosphorylcholine). In addition, the sodium ion transference number value of a ternary copolymer-supported ionogel electrolyte was determined to be larger compared to that of the ionic liquid solution (0.19 vs. 0.10, respectively).

Introduction

The development of new energy technologies has been propelled by fast-growing global energy consumption, as well as environmental issues that come with the burning of fossil fuels, such as air pollution and greenhouse gas emissions.¹ In order to fully leverage clean and renewable energy sources like solar or wind energy as substitutes, advanced energy storage devices are required. Safe, high energy density batteries are also desirable for wearable electronics and electric vehicles.²⁻⁴ Today, lithium-ion batteries (LIBs) dominate in the energy storage arena because of the small ionic radius of the lithium cation (0.76 Å), which promotes its rapid diffusion, and the light weight and high standard reduction potential of lithium (-3.04 V vs. SHE), which endow LIBs with large cell operating voltages and high energy densities.^{5,6} Increasing demand for LIBs, however, may lead to the shortage of lithium minerals in the near future, considering their limited sources and non-uniform distribution within the Earth's crust.^{7,8} Sodium, in contrast, is the sixth most mass-abundant element on Earth, and yet, it possesses very similar characteristics as lithium, including a small ionic radius (1.02 Å) and a high standard reduction potential (-2.71 V vs. SHE), which provides a compelling rationale to develop sodium-ion batteries (SIBs) as a possible alternative to LIBs.⁹⁻¹³ Typical SIB electrolytes under investigation comprise a sodium salt dissolved in an organic solvent such as carbonates and/or ethers, similar to what is used in many LIBs.⁹ However, safety concerns can arise from the flammability of such organic solvents and the

potential hazards of electrolyte leakage. One of the most promising methods to mitigate such safety risks would be to adopt a nonflammable liquid electrolyte or a solid-state electrolyte for SIBs.¹⁴⁻¹⁸

Ionic liquids (ILs), which are molten salts at or near room temperature, represent an appealing class of safer electrolyte materials for battery applications owing to their numerous unique properties such as nonflammability, negligible vapor pressure, wide liquid temperature range, and outstanding electrochemical and thermal stabilities.¹⁹⁻²¹ Wongittharom et al. investigated SIB performance using BMP TFSI electrolytes containing various NaTFSI concentrations (BMP: 1-butyl-1-methylpyrrolidinium, TFSI: bis(trifluoromethylsulfonyl)imide), demonstrating the nonflammability of the IL-based electrolytes and an increased cyclability of SIB prototypes that employed the IL electrolyte in comparison to those containing an organic solvent electrolyte.²² Ionogels, which are free-standing composites of ILs supported by a solid scaffold (such as a cross-linked polymer network), offer great promise for solid-state battery applications because of their mechanical flexibility, high room temperature ionic conductivity ($\sim 1\text{-}10\text{ mS cm}^{-1}$) and leakproof character.²³⁻²⁸ There have been many studies of various ionogel electrolytes for potential LIB applications to date, while only a few ionogel materials have been reported as candidate electrolytes specifically for SIBs.^{9,18,29-31} Noor and coworkers reported ionogel electrolytes based on a NaTFSI/BMP TFSI solution supported by either fumed silica or cross-linked poly(methyl methacrylate) (PMMA) as two different scaffold types for SIB applications.²⁹ It was observed that the room temperature ionic conductivities of the PMMA-supported ionogels ($< 1\text{ mS cm}^{-1}$) were decreased by at least 50% compared to that of the IL solution.²⁹ Recent collaborative reports from the Mecerreyes and Forsyth groups demonstrated ionogels for SIBs using cross-linked poly(ethylene glycol) diacrylate (PEGDA) scaffolds, which displayed improved ionic conductivities that were closer to those of their neat IL solutions.^{30,31}

Zwitterionic (ZI) polymers have emerged as a unique class of ionogel scaffold materials that can alleviate the typical gel trade-off between increased mechanical stiffness and decreased ionic conductivity. In a first study, Lind et al. found that ZI copolymer-supported ionogels displayed nearly constant room temperature ionic conductivity ($\sim 6.5 \text{ mS cm}^{-1}$) while the elastic modulus could be increased nearly 200-fold by introducing additional noncovalent dipole-dipole cross-links between ZI functional groups within the polymer chains, for a fixed small amount of covalent cross-linker.³² More recently, this group has demonstrated *fully-ZI* copolymer-supported ionogels (containing no covalent cross-links) featuring a neat IL,^{33,34} a solvate IL,³⁵ and a LiTFSI/IL solution.³⁶ Remarkably, an ionogel of 1M LiTFSI in BMP TFSI supported by a 12.5 wt.% fully-ZI copolymer scaffold exhibited both a high room temperature ionic conductivity ($> 1 \text{ mS cm}^{-1}$) and elastic modulus (up to 14 MPa), and also showed good promise as a solid-state electrolyte for LIBs.³⁶

In this report, ZI copolymer scaffolds have been employed for the first time to create ionogel electrolytes specifically designed for SIBs, using a 0.5M NaTFSI in BMP TFSI solution. Two different ZI monomers, sulfobetaine vinylimidazole (SBVI) and 2-methacryloyloxyethyl phosphorylcholine (MPC), were first combined in various molar ratios at the same total polymer content (15 mol%) in order to create ionogel electrolytes via *in situ* UV-initiated free radical copolymerization. The fully-ZI scaffold ionogels displayed excellent room temperature ionic conductivity ($> 1 \text{ mS cm}^{-1}$) and high elastic modulus ($\sim 10 \text{ MPa}$) across all formulations, which indicated the successful formation of noncovalent cross-links by both ZI moieties. Then, the ZI copolymer scaffold was “diluted” by copolymerization of both ZI monomers together with a third, non-ZI monomer: 2,2,2-trifluoroethyl methacrylate (TFEMA), in order to explore the effect of the non-ZI component on gel formation and resulting gel properties. Remarkably, robust and stiff

ionogels could still be obtained after greatly reducing the ZI fraction in the copolymer scaffold. For example, a freestanding ionogel with a compressive elastic modulus of 670 kPa was obtained by using a SBVI/MPC/TFEMA molar ratio of 1/1/3 at a total polymer content of 15 mol% (*i.e.* only 6 mol% ZI content in the gel). Temperature dependent ionic conductivity and nuclear magnetic resonance (NMR) spectroscopy measurements revealed favorable interactions between Na^+ cations and the ZI scaffold; however, distinct differences are seen compared to what was previously observed between such scaffolds and Li^+ cations. Lastly, a ZI copolymer scaffold exhibited an enhanced Na^+ transference number compared to the IL solution, which is desirable for future SIB applications.

Experimental Section

All materials were received and stored in a nitrogen-filled glove box (H_2O , $\text{O}_2 < 0.1$ ppm) until the time of use unless stated otherwise, and were used as received without further purification. The monomer 2-methacryloyloxyethyl phosphorylcholine (MPC, 97% purity), the photoinitiator, 2-hydroxy-2-methylpropiophenone (HOMPP), 2,2,2-trifluoroethyl methacrylate (TFEMA) and sodium metal (> 99.8%) were purchased from Sigma Aldrich. The ionic liquid, 1-butyl-1-methylpyrrolidinium bis(trifluoromethylsulfonyl)imide (BMP TFSI), was purchased from MilliporeSigma (High Purity grade). Sodium bis(trifluoromethylsulfonyl)imide (NaTFSI) was purchased from Solvionic (99.5% purity). The monomer sulfobetaine vinylimidazole (SBVI) was prepared according to a previously reported method.³² The neat liquid electrolyte was prepared by dissolving sufficient NaTFSI in BMP TFSI to create a 0.5M solution and stirred at 70 °C overnight inside the nitrogen-filled glove box until a homogenous, colorless liquid solution was obtained.

Ionogel precursor solutions were prepared by adding a desired quantity of monomers into the liquid electrolyte and stirring at 50 °C for up to 3 hours, until they were completely dissolved. Subsequently, 2 wt.% (total monomer basis) of HOMPP was added into the precursor solution and complete copolymerization was achieved *via* UV irradiation at 365 nm (Spectronic Corp., 8 W) for 5 min after the precursor was poured into a mold.

AC impedance spectroscopy was performed using a VersaSTAT 3 potentiostat with a built-in frequency response analyzer (Princeton Applied Research). Ionogel gel precursor solutions were poured into a custom-built Teflon cell array with gold-coated electrode pins, polymerized *in situ*, and rested for 24 hours inside the nitrogen-filled glove box. Room temperature (22 °C) AC impedance spectroscopy measurements were conducted inside the nitrogen-filled glove box over the frequency range of 1 Hz to 100 kHz using a sinusoidal voltage amplitude of 10 mV (0 V DC offset). The cell constant used to convert the impedance value at high frequency (~100 kHz) to an ionic conductivity was determined by calibration using three different neat ionic liquid electrolytes with known conductivity values. At least three replicate ionogel samples were prepared for each formulation, and average values were calculated to determine the ionic conductivity. Temperature-dependent ionic conductivity measurements were performed using a Linkam Scientific Instruments LTS 420 temperature-controlled, nitrogen-filled microscopy stage. Impedance spectra were recorded between 10 °C and 80 °C with a 20 min hold for thermal equilibration at each point.

Ionogel mechanical characterization was performed by compression testing in free-extension mode using an ARES-LS2 rheometer (TA Instruments) in ambient laboratory conditions, from 0% to a minimum of 12% strain with a platen travel rate of 0.01 mm s⁻¹. Elastic modulus values were obtained as the slope of the linear stress-strain curve region at low strain values

(Supporting Information, Figure S1). Cylindrical-shaped ionogels were created for mechanical characterization (diameter = 6.4 mm, thickness = 3.2 mm).

^{23}Na and ^{19}F NMR spectroscopy measurements were performed using a Bruker AVANCE III 500 MHz spectrometer. A total of 16 scans were recorded at room temperature with a relaxation delay of 10 ms. A reference solution (0.1M NaTFSI in D_2O) was injected into a glass capillary tube (inner diameter 1.5 mm) and subsequently placed inside of a 5 mm inner diameter standard NMR tube filled with the electrolyte solution of interest.

Sodium transference numbers were determined using the method of Evans et al.³⁷ Na|electrolyte|Na symmetrical cells were assembled using a custom Swagelok-type test apparatus inside the nitrogen-filled glove box. DC polarization/chronoamperometry was performed using an applied potential of 40 mV. Additional details can be found in the Supporting Information.

Linear sweep voltammetry (LSV) was performed using a type 304 stainless steel working electrode|electrolyte|Na configuration using CR2032 coin cells (MTI Corp.) assembled inside an argon-filled glove box. Both the NaTFSI/BMP TFSI liquid and ionogel precursor solution were loaded into *Celgard* separator films (25 μm thick, MTI Corp.) via vacuum infiltration overnight, followed by UV irradiation of the latter as described above. LSV was performed using a VersaSTAT 3 potentiostat (Princeton Applied Research) at a sweep rate of 1 mV s^{-1} in the anodic direction.

Results and Discussion

A series of ionogel electrolyte samples was synthesized by *in situ* UV-initiated free radical copolymerization of the ZI co-monomers SBVI and MPC, together with the non-ZI monomer TFEMA in some cases, inside a previously-studied ionic liquid-based electrolyte for SIBs: a 0.5M

solution of NaTFSI in BMP TFSI (Na/IL) solution.²² Figure 1a displays the molecular structure of the linear copolymer scaffold, comprised of SBVI, MPC, and TFEMA monomer units. Two photographs of representative 15 mol.% copolymer-supported ionogel samples are shown in Figure 1b, which demonstrate that freestanding and transparent gels were successfully obtained. It should be noted that all of the ionogel formulations in this study shared the same total copolymer content of 15 mol.%, within which the relative molar ratios of SBVI/MPC/TFEMA were varied. The creation of freestanding gels without introducing any covalent cross-links demonstrates the facile formation of dipole-dipole ZI functional group cross-links between copolymer chains in the Na/IL solution, similar to what was previously reported in a Li/IL system.³⁶

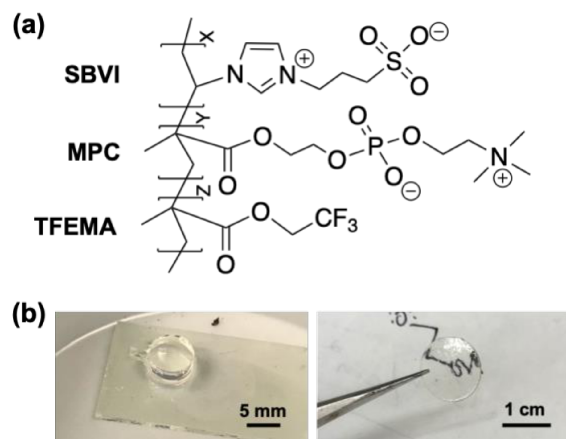


Figure 1. (a) Molecular structure of the copolymer scaffolds used in this work, comprising various molar ratios of sulfobetaine vinylimidazole (SBVI), 2-methacryloyloxyethyl phosphorylcholine (MPC), and 2,2,2-trifluoroethyl methacrylate (TFEMA) monomer subunits. (b) Photographs of representative 15 mol.% copolymer-supported, 0.5M NaTFSI/BMP TFSI ionogel samples; both gels contain a SBVI/MPC/TFEMA molar ratio of 1/1/3. Left image: freestanding cylindrical gel (6.4 mm diameter, 3.2 mm height) on a glass slide; right image: circular disc-shaped gel (~1 mm thick) held with tweezers in front of a pen-and-paper drawing to show its optical transparency.

AC impedance spectroscopy and compressive stress-strain testing were performed in order to assess the ionic conductivity and compressive elastic modulus, respectively, of each gel sample. Figure 2a displays both the elastic modulus and ionic conductivity values for four fully-ZI copolymer-supported ionogel electrolyte formulations possessing different molar ratios between the SBVI and MPC subunits (1/3, 1/2, 1/1, and 2/1). The room temperature ionic conductivities of these ionogels were found to be fairly consistent at approximately 1.4-1.6 mS cm⁻¹. Notably, all four of these gel electrolytes exhibited higher ionic conductivities than that of the neat Na/IL liquid electrolyte (1.2 ± 0.1 mS cm⁻¹), similar to what was previously observed for Li/IL gel analogues,³⁶ which is consistent with our hypothesis that ZI polymer functional groups can promote additional dissociation of ion pairs/clusters within IL systems.¹⁸ It was also seen that the compressive elastic moduli of the Na/IL gel samples (approximately 7-11 MPa, Fig. 2a) were comparable to those of fully-ZI copolymer-supported Li/IL gel electrolytes (*e.g.* 14 MPa for a 1/3 SBVI/MPC molar ratio in 1M LiTFSI/BMP TFSI at 17 mol% copolymer),³⁶ which provided evidence that robust physical cross-links between ZI functional groups on the polymer chains could also be achieved in the Na/IL solution environment. Importantly, variation of the SBVI/MPC molar ratio did not result in substantial changes in the elastic modulus of Na/IL ionogels. This stands in stark contrast to what was observed for Li/IL ionogels, for which gel stiffnesses showed a clear and monotonic increase as the molar fraction of SBVI in the fully-ZI scaffold was increased.³⁶ Therefore, an important difference between the Na/IL system studied here and the Li/IL system appears to be the ability of both SBVI and MPC subunits to contribute somewhat equally to the formation of noncovalent cross-links in Na/IL ionogels, while SBVI is the predominant cross-linker in Li/IL gels.

Given the high stiffness of the fully-ZI scaffold gel formulations, it stood to reason that these linear copolymers could likely be “diluted” by including a third, non-ZI subunit that would

effectively space out the ZI groups, yet still enable robust, free-standing gel electrolytes. Clearly, every single ZI group of a fully-ZI scaffold cannot participate simultaneously in forming noncovalent cross-links to build the gel scaffold network. Therefore, a question was posed: what happens to ionogel stiffness and ionic conductivity as the fraction of copolymer that is non-ZI is increased? In order to begin to answer this, ternary copolymer scaffolds were synthesized by *in situ* copolymerization of SBVI, MPC, and a non-ZI component, TFEMA, within the Na/IL electrolyte. The SBVI/MPC molar ratio was fixed at 1/1 while the molar fraction of TFEMA in the scaffold was varied, since the 1/1 fully-ZI gel displayed the highest stiffness (11 MPa, Fig. 2a).

The properties of these three additional ionogel formulations, having SBVI/MPC/TFEMA molar ratios of 1/1/1, 1/1/2, and 1/1/3, are shown in Figure 2b. It should be noted that all three of the gel samples also featured a total copolymer content of 15 mol% and were transparent and freestanding. Freestanding gels could not be obtained, however, when the TFEMA fraction was increased beyond 60 mol% (*i.e.* SBVI/MPC/TFEMA = 1/1/3) within the copolymer. Room temperature ionic conductivities of the three ionogels containing TFEMA subunits (1.4-1.6 mS cm⁻¹) remained higher than the Na/IL solution and comparable to those of the gels with fully-ZI scaffolds. This indicated that the ZI content within the copolymer scaffold could be reduced to at least 40 mol% while retaining the benefits of additional ion pair/cluster dissociation for this electrolyte. As expected, the compressive elastic modulus was observed to decrease as the TFEMA content increased (Fig. 2b), dropping from 5.3 MPa for the 1/1/1 scaffold (33 mol% TFEMA) down to 0.7 MPa for the 1/1/3 scaffold (60 mol% TFEMA). The monotonic decrease of gel elastic modulus as the fraction of the non-ZI subunit was increased can be understood by a decrease in the noncovalent ZI cross-link density, which softened the gel electrolytes. The lowest elastic modulus reported here (0.7 MPa), for the ionogel with the highest TFEMA content (1/1/3 scaffold),

is still significantly higher than that displayed by a comparable Li/IL ionogel at its gelation point (*i.e.* minimum scaffold required to obtain a freestanding gel), ~ 0.01 MPa.³⁶

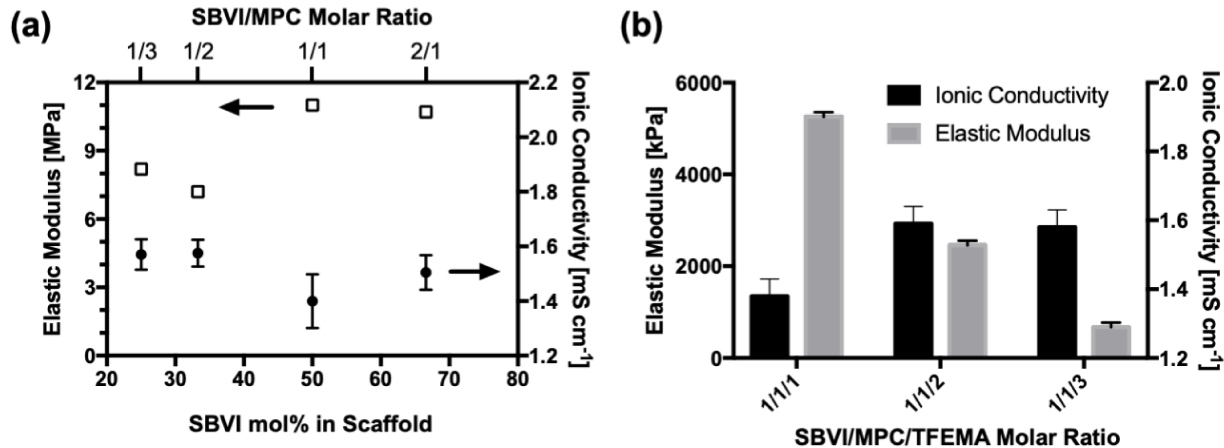


Figure 2. (a) Compressive elastic modulus values (open squares, left axis) and room temperature ionic conductivity values (filled circles, right axis) of ionogel electrolytes with fully-ZI scaffolds plotted versus SBVI mol% within the copolymer scaffold. (b) Compressive elastic modulus and room temperature ionic conductivity values of ionogel electrolytes with “diluted” ternary copolymer scaffolds containing TFEMA subunits. All ionogel samples have a total copolymer content of 15 mol% (85 mol% Na/IL solution).

Figure 3 depicts the temperature dependence of ionic conductivity measured from 10 °C to 80 °C for three representative samples: the Na/IL solution, a fully-ZI copolymer-supported ionogel electrolyte (SBVI/MPC molar ratio of 1/1), and a ternary copolymer-supported ionogel electrolyte (SBVI/MPC/TFEMA molar ratio of 1/1/3). The gel samples remained freestanding and did not show any liquid leakage throughout the entire temperature range. The activation energy of ionic conductivity (E_A) values were calculated via a simple Arrhenius model fit. It could be observed that the activation energy values were approximately 23 ± 1 kJ mol⁻¹ for both the Na/IL solution

and the ternary copolymer gel electrolyte, while a lower E_A value of $18 \pm 1 \text{ kJ mol}^{-1}$ was determined for the gel with the fully-ZI copolymer scaffold. Polymer-supported ionogel electrolytes typically exhibit larger E_A values compared to that of their base liquid electrolyte, due both to a reduction in ionic charge carrier density (the polymer is nonconductive) and hindered ion mobility through the scaffold network.³⁸ However, the fully-ZI copolymer scaffold promotes enhanced ion transport through $\text{Li}^+ \cdots \text{ZI}$ functional group interactions that results in a lower E_A value for the ionogel; the same phenomenon was also observed previously in the Li/IL system.³⁶ The similar E_A values displayed by both the neat Na/IL solution and the ternary copolymer-supported gel electrolyte can also be explained by an ionic conductivity enhancement effect due to the ZI functional groups. The expected increase in gel E_A due to the presence of non-ZI TFEMA (60 mol% of this scaffold) was effectively compensated for by the enhancement of the ZI groups (40 mol% of this scaffold), such that the ternary copolymer scaffold gel electrolyte exhibited a very similar E_A value to that of the neat Na/IL solution.

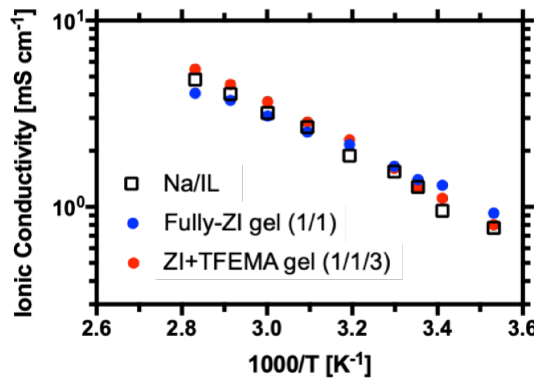


Figure 3. Temperature dependence of ionic conductivity measured between 10 °C and 80 °C for the 0.5M NaTFSI-BMP TFSI liquid electrolyte (Na/IL), an ionogel electrolyte with a fully-ZI scaffold (SBVI/MPC molar ratio of 1/1, total polymer content of 15 mol%), and an ionogel electrolyte with a ternary copolymer scaffold (SBVI/MPC/TFEMA molar ratio of 1/1/3, total polymer content of 15 mol%).

Further insights into interactions between the various copolymer subunits and the ions of the Na/IL solution were obtained by analyzing the chemical shifts of the ^{23}Na and ^{19}F nuclei via NMR spectroscopy, focusing attention on the signals attributed to the Na^+ and TFSI^- ions, respectively. All of the chemical shifts were measured in monomer solutions, rather than in ionogel samples, in order to observe the effects of each monomer individually. Solutions (5 mol% monomer) were prepared in the Na/IL liquid electrolyte, and ^{23}Na and ^{19}F NMR spectra were recorded, as shown in Figure 4. Figure 4a compares the ^{23}Na spectra for solutions containing 5 mol% of each monomer (MPC, SBVI, or TFEMA) to the Na/IL solution (0.5M NaTFSI/BMP TFSI). It can be seen that the 5 mol% TFEMA solution shares essentially the same ^{23}Na peak position as the Na/IL solution, which indicates that TFEMA does not strongly interact with the Na^+ cations. However, for both of the 5 mol% ZI monomer solutions, SBVI and MPC, a similar downfield shift in the ^{23}Na peak position was observed in comparison to the Na/IL peak position, moving from approximately -11.5 ppm to -10.9 ppm. This provides clear evidence of attractive interactions that exist between both ZI types and Na^+ cations, which changes their local electronic environment (*i.e.* ZI groups can displace TFSI^- in the first coordination shell with Na^+). A similar phenomenon was reported in the Li/IL system, although the magnitude of the chemical shift change was much larger for MPC with Li^+ compared to that of SBVI.³⁶ Therefore, an important finding of this study is that both SBVI and MPC appear to interact comparably with Na^+ in the Na/IL environment, which stands in contrast to the different behaviors of SBVI and MPC in the Li/IL solution. This result is also consistent with the nearly unchanged ionogel elastic modulus values that were observed as the SBVI/MPC molar ratio was varied within a fully-ZI copolymer scaffold (Fig. 2a).

The sharper and well-defined ^{19}F spectra (all normalized to the same height) shown in Figure 4b, measured using the same solutions, allow one to understand the different monomer-ion interactions from another perspective. The ^{19}F spectrum of the IL alone (BMP TFSI) was also measured, so that the local TFSI $^-$ environments in the neat IL versus the Na/IL solution could be compared. The spectrum of neat BMP TFSI displayed a peak at -80.07 ppm, which represents the local environment of TFSI $^-$ coordinated with the IL cation, BMP $^+$. The addition of 0.5M NaTFSI to the IL causes an upfield peak shift, from -80.07 ppm to -80.32 ppm, which indicates the presence of Na $^+$...TFSI $^-$ interactions in the Na/IL solution. When 5 mol% of SBVI or MPC monomers are included, they induce downfield peak shifts to -80.24 and -80.2 ppm, respectively. These shifts reflect the favorable ZI...Na $^+$ interactions observed in the ^{23}Na spectra, which effectively draw Na $^+$ cations away from TFSI $^-$, allowing more of the anions to return to their original pairings with BMP $^+$. In contrast, the 5 mol% TFEMA solution showed very little shift in the ^{19}F peak position compared to the Na/IL solution, reinforcing the notion that TFEMA is essentially a non-interacting monomer with respect to either the Na $^+$ or TFSI $^-$ ions in comparison to the zwitterions.

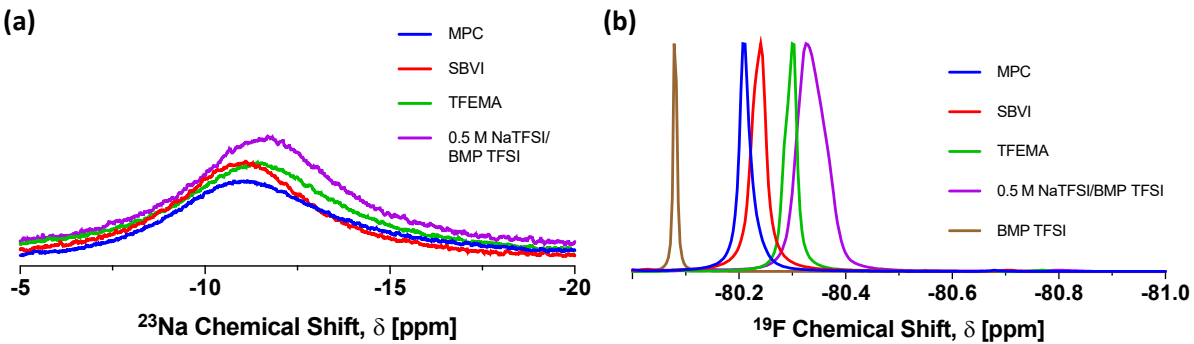


Figure 4. (a) ^{23}Na NMR spectra of solutions containing 5 mol% monomer (either MPC, SBVI, or TFEMA) in 0.5M NaTFSI/BMP TFSI, as well as that of the liquid electrolyte itself. (b) Normalized ^{19}F NMR spectra of the same solutions shown in panel (a), in addition to that of the neat ionic liquid (BMP TFSI).

Finally, the Na^+ transference number (t_{Na^+} , the fraction of total steady-state current carried by Na^+ cations) and anodic stability of a ZI copolymer-supported ionogel were examined and compared with those of the Na/IL solution. The ionogel with a ternary copolymer scaffold (SBVI/MPC/TFEMA molar ratio of 1/1/3, total copolymer content of 15 mol%) was selected, as this formulation both effectively reduces the amount of ZI monomers required (which are more expensive than TFEMA) and it displayed better chemical stability against the sodium metal electrodes compared to an ionogel having a fully-ZI copolymer scaffold (data not shown). Chronoamperometry tests were conducted using symmetrical $\text{Na}|\text{electrolyte}|\text{Na}$ cells with an applied potential of 40 mV in order to determine t_{Na^+} values; the normalized current responses for the two electrolytes are shown in Figure 5a. The ternary copolymer-supported (ZI+TFEMA gel) electrolyte exhibited a larger t_{Na^+} value (0.19) than that of the Na/IL liquid (0.10); see the Supporting Information for details regarding t_{Na^+} calculation. This finding suggests that the presence of ZI functional groups within the copolymer scaffold can, in fact, improve Na^+ cation transport, as was also observed in the Li/IL system.³⁶ Figure 5b shows the linear sweep voltammetry data measured for these two electrolytes (liquid solution and ionogel), measured using a stainless steel working electrode with a scan rate of 1 mV s⁻¹. Both the Na/IL solution and the ZI+TFEMA gel demonstrate excellent anodic stability up to at least ~5.5 V vs. Na/Na^+ . Collectively, these results demonstrate the strong potential of ZI copolymer-supported ionogel electrolytes for future SIB applications.

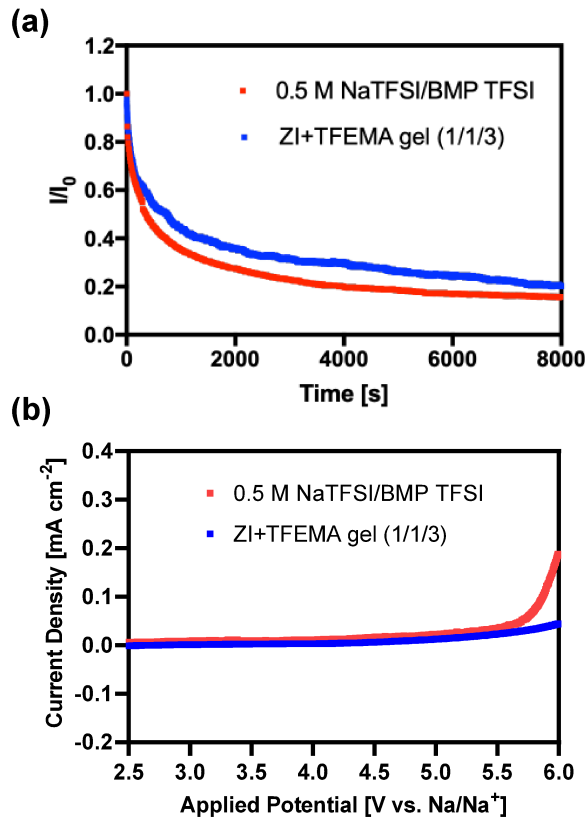


Figure 5. (a) Chronoamperometry responses of the 0.5M NaTFSI-BMP TFSI liquid electrolyte and of an ionogel electrolyte with a ternary copolymer scaffold (SBVI/MPC/TFEMA molar ratio of 1/1/3, total polymer content of 15 mol%) to an applied potential of 40 mV, measured in symmetric Na|electrolyte|Na cells. (b) Linear sweep voltammograms (1 mV s^{-1}) of the 0.5M NaTFSI-BMP TFSI liquid electrolyte and of an ionogel electrolyte with a ternary copolymer scaffold (SBVI/MPC/TFEMA molar ratio of 1/1/3, total polymer content of 15 mol%), measured in stainless steel (working electrode)|electrolyte|Na cells.

Conclusions

In summary, ZI copolymers were successfully employed to create a series of novel Na⁺ cation-conducting ionogel electrolytes. Both of the ZI monomer moieties (sulfobetaine of SBVI and phosphorylcholine of MPC) readily formed noncovalent cross-links within the nonaqueous

NaTFSI/BMP TFSI electrolyte environment, leading to stiff ionogels (elastic modulus values \sim 10 MPa) with a total copolymer content of only 15 mol%. Both zwitterions displayed similarly attractive interactions with Na^+ cations, as revealed by NMR chemical shift analysis. Copolymerization of a 1/1 molar ratio mixture of SBVI/MPC together with a third, non-ZI monomer (TFEMA) also enabled the formation of freestanding ionogels. These “diluted” ZI linear copolymers represent a new approach to ionogel formation, which allows for further tunability of gel properties and conservation of the more expensive ZI monomers. Compared to a fully-ZI copolymer-supported gel electrolyte (SBVI/MPC molar ratio of 1/1), a ternary copolymer-supported ZI+TFEMA gel electrolyte (SBVI/MPC/TFEMA molar ratio of 1/1/3) displayed a higher activation energy of ionic conductivity, but its activation energy was still not higher than that of the Na/IL electrolyte itself. The ZI+TFEMA scaffold also provided an enhancement of the sodium ion transference number compared to that of the neat Na/IL solution. This study has revealed key differences regarding how these two particular ZI functional groups interact with the alkali metal cations within Na/IL versus Li/IL electrolytes, and it has introduced the design of a new class of ZI copolymer scaffolds for future ionic liquid-based gel polymer electrolytes in general.

Acknowledgements

The authors gratefully acknowledge Daxian Cao and Prof. Hongli Zhu from Northeastern University for helpful discussions and for providing the sodium metal. The authors also thank Morgan Taylor for assistance in collecting the linear sweep voltammetry data. This work was performed with support from the National Science Foundation (CBET-1802729) and from Tufts University.

Supporting Information

Ionogel scaffold formulation details, representative ionogel compressive stress-strain data, a description of the sodium ion transference number measurements, including Nyquist plots recorded before/after polarization (PDF)

References

- (1) Nocera, D. G., Living Healthy on a Dying Planet. *Chem. Soc. Rev.* **2009**, *38*, 13–15.
- (2) Larcher, D.; Tarascon, J. M., Towards Greener and More Sustainable Batteries for Electrical Energy Storage. *Nat. Chem.* **2015**, *7*, 19–29.
- (3) Bruce, P. G.; Freunberger, S. A.; Hardwick, L. J.; Tarascon, J. M., Li-O₂ and Li-S Batteries with High Energy Storage. *Nat. Mater.* **2012**, *11*, 19–29.
- (4) Liu, W.; Song, M. S.; Kong, B.; Cui, Y., Flexible and Stretchable Energy Storage: Recent Advances and Future Perspectives. *Adv. Mater.* **2017**, *29*, 1603436.
- (5) Dunn, B.; Kamath, H.; Tarascon, J. M., Electrical Energy Storage for the Grid: A Battery of Choices. *Science* **2011**, *334*, 928–935.
- (6) Etacheri, V.; Marom, R.; Elazari, R.; Salitra, G.; Aurbach, D., Challenges in the Development of Advanced Li-Ion Batteries: A Review. *Energy Environ. Sci.* **2011**, *4*, 3243–3262.
- (7) Tarascon, J. M., Is Lithium the New Gold? *Nat. Chem.* **2010**, *2*, 510.
- (8) Hwang, J. Y.; Myung, S. T.; Sun, Y. K., Sodium-Ion Batteries: Present and Future. *Chem. Soc. Rev.* **2017**, *46*, 3529–3614.
- (9) Ponrouch, A.; Monti, D.; Boschin, A.; Steen, B.; Johansson, P.; Palacín, M. R., Non-

- Aqueous Electrolytes for Sodium-Ion Batteries. *J. Mater. Chem. A* **2015**, *3*, 22–42.
- (10) Pan, H.; Hu, Y. S.; Chen, L., Room-Temperature Stationary Sodium-Ion Batteries for Large-Scale Electric Energy Storage. *Energy Environ. Sci.* **2013**, *6*, 2338–2360.
- (11) Forsyth, M.; Yoon, H.; Chen, F.; Zhu, H.; MacFarlane, D. R.; Armand, M.; Howlett, P. C., Novel Na^+ Ion Diffusion Mechanism in Mixed Organic–Inorganic Ionic Liquid Electrolyte Leading to High Na^+ Transference Number and Stable, High Rate Electrochemical Cycling of Sodium Cells. *J. Phys. Chem. C* **2016**, *120*, 4276–4286.
- (12) Terada, S.; Mandai, T.; Nozawa, R.; Yoshida, K.; Ueno, K.; Tsuzuki, S.; Dokko, K.; Watanabe, M., Physiochemical Properties of Pentaglyme–Sodium Bis(trifluoromethanesulfonyl)amide Solvate Ionic Liquid. *Phys. Chem. Chem. Phys.* **2014**, *16*, 11737–11746.
- (13) Kundu, D.; Talaie, E.; Duffort, V.; Nazar, L. F., The Emerging Chemistry of Sodium Ion Batteries for Electrochemical Energy Storage. *Angew. Chem. Int. Ed.* **2015**, *54*, 3431–3448.
- (14) Sun, Y.; Shi, P.; Xiang, H.; Liang, X.; Yu, Y., High-Safety Nonaqueous Electrolytes and Interphases for Sodium-Ion Batteries. *Small* **2019**, *15*, 1–17.
- (15) Lu, Y.; Li, L.; Zhang, Q.; Niu, Z.; Chen, J., Electrolyte and Interface Engineering for Solid-State Sodium Batteries. *Joule* **2018**, *2*, 1747–1770.
- (16) Xie, M.; Li, S.; Huang, Y.; Wang, Z.; Jiang, Y.; Wang, M.; Wu, F.; Chen, R., An Ionic Liquid/Poly(vinylidene fluoride-co-hexafluoropropylene) Gel–Polymer Electrolyte with a Compatible Interface for Sodium-Based Batteries. *ChemElectroChem* **2019**, *6*, 2423–2429.
- (17) Mendes, T. C.; Zhang, X.; Wu, Y.; Howlett, P. C.; Forsyth, M.; MacFarlane, D. R.,

- Supported Ionic Liquid Gel Membrane Electrolytes for a Safe and Flexible Sodium Metal Battery. *ACS Sustainable Chem. Eng.* **2019**, *7*, 3722–3726.
- (18) Forsyth, M.; Porcarelli, L.; Wang, X.; Goujon, N.; Mecerreyes, D., Innovative Electrolytes Based on Ionic Liquids and Polymers for Next-Generation Solid-State Batteries. *Acc. Chem. Res.* **2019**, *52*, 686–694.
- (19) Watanabe, M.; Thomas, M. L.; Zhang, S.; Ueno, K.; Yasuda, T.; Dokko, K., Application of Ionic Liquids to Energy Storage and Conversion Materials and Devices. *Chem. Rev.* **2017**, *117*, 7190–7239.
- (20) Galinski, M.; Lewandowski, A.; Stepniak, I., Ionic Liquids as Electrolytes. *Electrochim. Acta* **2006**, *51*, 5567–5580.
- (21) Matsumoto, K.; Hwang, J.; Kaushik, S.; Chen, C.; Hagiwara, R., Advances in Sodium Secondary Batteries Utilizing Ionic Liquid Electrolytes. *Energy Environ. Sci.* **2019**, *12*, 3247–3287.
- (22) Wongittharom, N.; Lee, T. C.; Wang, C. H.; Wang, Y. C.; Chang, J. K., Electrochemical Performance of Na/NaFePO₄ Sodium-Ion Batteries with Ionic Liquid Electrolytes. *J. Mater. Chem. A* **2014**, *2*, 5655–5661.
- (23) Le Bideau, J.; Viau, L.; Vioux, A., Ionogels, Ionic Liquid Based Hybrid Materials. *Chem. Soc. Rev.* **2011**, *40*, 907–925.
- (24) MacFarlane, D. R.; Forsyth, M.; Howlett, P. C.; Kar, M.; Passerini, S.; Pringle, J. M.; Ohno, H.; Watanabe, M.; Yan, F.; Zheng, W.; Zhang, S.; Zhang, J., Ionic Liquids and Their Solid-State Analogues as Materials for Energy Generation and Storage. *Nat. Rev. Mater.* **2016**, *1*, 15005.
- (25) Lee, J. H.; Lee, A. S.; Lee, J. C.; Hong, S. M.; Hwang, S. S.; Koo, C. M., Hybrid Ionogel

Electrolytes for High Temperature Lithium Batteries. *J. Mater. Chem. A* **2015**, *3*, 2226–2233.

- (26) Li, X.; Li, S.; Zhang, Z.; Huang, J.; Yang, L.; Hirano, S., High-Performance Polymeric Ionic Liquid-Silica Hybrid Ionogel Electrolytes for Lithium Metal Batteries. *J. Mater. Chem. A* **2016**, *4*, 13822–13829.
- (27) Guo, P.; Su, A.; Wei, Y.; Liu, X.; Li, Y.; Guo, F.; Li, J.; Hu, Z.; Sun, J., Healable, Highly Conductive, Flexible, and Nonflammable Supramolecular Ionogel Electrolytes for Lithium-Ion Batteries. *ACS Appl. Mater. Interfaces* **2019**, *11*, 19413–19420.
- (28) Lee, A. S.; Lee, J. H.; Hong, S. M.; Lee, J. C.; Hwang, S. S.; Koo, C. M., Boronic Ionogel Electrolytes to Improve Lithium Transport for Li-Ion Batteries. *Electrochim. Acta* **2016**, *215*, 36–41.
- (29) Noor, S. A. M.; Yoon, H.; Forsyth, M.; MacFarlane, D. R., Gelled Ionic Liquid Sodium Ion Conductors for Sodium Batteries. *Electrochim. Acta* **2015**, *169*, 376–381.
- (30) De Anastro, A. F.; Porcarelli, L.; Hilder, M.; Berlanga, C.; Galceran, M.; Howlett, P.; Forsyth, M.; Mecerreyes, D., UV-Cross-Linked Ionogels for All-Solid-State Rechargeable Sodium Batteries. *ACS Appl. Energy Mater.* **2019**, *2*, 6960–6966.
- (31) Ha, T. A.; De Anastro, A. F.; Ortiz-Vitoriano, N.; Fang, J.; MacFarlane, D. R.; Forsyth, M.; Mecerreyes, D.; Howlett, P. C.; Pozo-Gonzalo, C., High Coulombic Efficiency Na—O₂ Batteries Enabled by a Bilayer Ionogel/Ionic Liquid. *J. Phys. Chem. Lett.* **2019**, *10*, 7050–7055.
- (32) Lind, F.; Rebollar, L.; Bengani-Lutz, P.; Asatekin, A.; Panzer, M. J., Zwitterion-Containing Ionogel Electrolytes. *Chem. Mater.* **2016**, *28*, 8480–8483.
- (33) Taylor, M. E.; Lounder, S. J.; Asatekin, A.; Panzer, M. J., Synthesis and Self-Assembly of

- Fully Zwitterionic Triblock Copolymers. *ACS Materials Lett.* **2020**, *2*, 261–265.
- (34) Taylor, M. E.; Panzer, M. J., Fully-Zwitterionic Polymer-Supported Ionogel Electrolytes Featuring a Hydrophobic Ionic Liquid. *J. Phys. Chem. B* **2018**, *122*, 8469–8476.
- (35) D'Angelo, A. J.; Panzer, M. J., Design of Stretchable and Self-Healing Gel Electrolytes via Fully Zwitterionic Polymer Networks in Solvate Ionic Liquids for Li-Based Batteries. *Chem. Mater.* **2019**, *31*, 2913–2922.
- (36) D'Angelo, A. J.; Panzer, M. J., Decoupling the Ionic Conductivity and Elastic Modulus of Gel Electrolytes: Fully Zwitterionic Copolymer Scaffolds in Lithium Salt/Ionic Liquid Solutions. *Adv. Energy Mater.* **2018**, *8*, 1801646.
- (37) Evans, J.; Vincent, C. A.; Bruce, P. G., Electrochemical Measurement of Transference Numbers in Polymer Electrolytes. *Polymer* **1987**, *28*, 2324–2328.
- (38) D'Angelo, A. J.; Grimes, J. J.; Panzer, M. J., Deciphering Physical Versus Chemical Contributions to the Ionic Conductivity of Functionalized Poly(methacrylate)-Based Ionogel Electrolytes. *J. Phys. Chem. B* **2015**, *119*, 14959–14969.

Table of Contents (TOC) Image

